https://doi.org/10.15407/ujpe68.12.816

Y.M. AZHNIUK,[1] A.V. GOMONNAI,[1,2] V.V. LOPUSHANSKY,[1] O.O. GOMONNAI,[2] T. BABUKA,[2] V.Y. LOYA,[1] I.M. VOYNAROVYCH[1]

[1] Institute of Electron Physics, Nat. Acad. of Sci. of Ukraine
*(21, Universytets'ka Str., Uzhhorod 88017, Ukraine; e-mail: yu.azhniuk@gmail.com)*
[2] Uzhhorod National University
*(3, Narodna Sq., Uzhhorod 88000, Ukraine)*

# LASER-INDUCED TRANSFORMATIONS IN THERMALLY EVAPORATED THIN $TlInSe_2$ FILMS STUDIED BY RAMAN SPECTROSCOPY

*$TlInSe_2$ films with thickness from 10 to 200 nm were thermally evaporated on silicon and silicate glass substrates. Micro-Raman spectra measured at a moderate excitation (532 nm, 4 kW/cm$^2$) confirm the amorphous character of the films. Narrow features revealed in the spectra at an excitation power density of 40 kW/cm$^2$ show the evidence for the formation of $TlInSe_2$, TlSe, and $In_2Se_3$ crystallites in the laser spot. For thin (10–30 nm) films, the rod-shaped $TlInSe_2$ crystallites are shown to be oriented within the film plane. The crystallite formation is governed by the thermal effect of the tightly focused laser beam.*

*Keywords*: thin films, thermal evaporation, Raman spectroscopy, crystallisation.

## 1. Introduction

$TlInSe_2$ is a rather well-known semiconductor material with chain-like structure (tetragonal crystal system) [1]. It is extensively studied [2–9], in particular, in view of possible phase transitions (which are still questionable) [10, 11, & references therein]. It is sometimes referred to as a quasi-one-dimensional or one-dimensional (1-D) material [4], and several publications were devoted to the properties of nanoscale (30–50 nm) $TlInSe_2$ structures [3, 12]. Properties of $TlInSe_2$ make it promising for applications in acoustooptics [11], electronics [13], thermoelectricity [3, 9], neutron and $\gamma$-ray detection [7]. Important information about the crystal structure and lattice dynamics of $TlInSe_2$ can be gained from Raman spectroscopy [2, 5, 8, 14, 15].

In the recent years, an additional research interest toward thin $TlInSe_2$ films emerged [16, 17], similarly to the films of related I–III–$VI_2$ materials prepared mostly by the thermal evaporation [18–26].

Here, we present a Raman spectroscopic study of structural transformations in thermally evaporated thin $TlInSe_2$ films under the illumination by a tightly focused laser beam.

## 2. Experimental

$TlInSe_2$ films with thickness $d$ from 10 to 200 nm were prepared by the thermal evaporation of presynthesised crystalline $TlInSe_2$ (the synthesis details can be found elsewhere [14]) on silicon and silicate

Citation: Azhniuk Y.M., Gomonnai A.V., Lopushansky V.V., Gomonnai O.O., Babuka T., Loya V.Y., Voynarovych I.M. Laser-induced transformations in thermally evaporated thin $TlInSe_2$ films studied by Raman spectroscopy. *Ukr. J. Phys.* **68**, No. 12, 816 (2023). https://doi.org/10.15407/ujpe68.12.816.

Цитування: Ажнюк Ю., Гомоннай О.В., Лопушанський В., Гомоннай О.О., Бабука Т., Лоя В., Войнарович І. Раманівське дослідження індукованих лазерним випромінюванням перетворень у термічно напилених тонких плівках $TlInSe_2$. *Укр. фіз. журн.* **68**, №12, 818 (2023).

glass substrates at room temperature at a pressure of $\sim 2\times10^{-4}$ Pa with an evaporation rate of 4 nm/s. The evaporation temperature was 1050 K. The thickness of the films was roughly estimated by interferometry (for the thicker films) and by interpolation with the account for the evaporation time (for the thinner samples).

Micro-Raman scattering measurements were carried out at room temperature using an XPloRa Plus spectrometer (Horiba). Excitation was provided by a solid-state laser ($\lambda_{exc} = 532$ nm). The scattered light was detected by a cooled CCD camera. The instrumental resolution was better than 2.5 $cm^{-1}$.

## 3. Results and Discussion

Raman spectra of $TlInSe_2$ films on silicate glass and silicon substrates measured at a low excitation power density ($P_{exc} = 4$ kW/$cm^2$) are shown in Fig. 1. The features in the spectra are noticeably broader than for single-crystal $TlInSe_2$ [8, 14]. Hence, the films can be treated as amorphous. The half-width of the most intense maximum near 165 $cm^{-1}$ is in the interval 20–35 $cm^{-1}$ for the films evaporated on the glass substrate and 15–35 $cm^{-1}$ for the films on the silicon substrate. While for the samples on the glass substrate there is no clear dependence of the band half-width on the film thickness, for those on the silicon substrate a trend of the peak narrowing with the film thickness is observed.

In our opinion, an even clearer evidence of the amorphous structure of the films is the frequency position of the most intense peak (near 165 $cm^{-1}$) which, for $TlInSe_2$, should be expected near 180–185 $cm^{-1}$. Note that a recent study performed for thermally evaporated polycrystalline $TlInSe_2$ films clearly revealed the dominant Raman peak at 181 $cm^{-1}$ and a less intense feature at 169 $cm^{-1}$ [17]. Likewise, the spectrum of single-crystal $TlInSe_2$ in $Z(XX+XY)\bar{Z}$ scattering configuration exhibits the most prominent narrow peak at 185 $cm^{-1}$, a less intense maximum at 171 $cm^{-1}$, and an even weaker shoulder near 200 $cm^{-1}$ (Fig. 2). Similar spectra were observed for single-crystalline $TlInSe_2$ in earlier studies [8, 14]. The most intense feature corresponds to fully symmetric vibrations of $A_{1g}$ symmetry, while the features at 173 $m^{-1}$ and 205 $cm^{-1}$ (see the inset in Fig. 2) are attributed to vibrations of $E_g$ and $E_u$ symmetry, respectively [8].

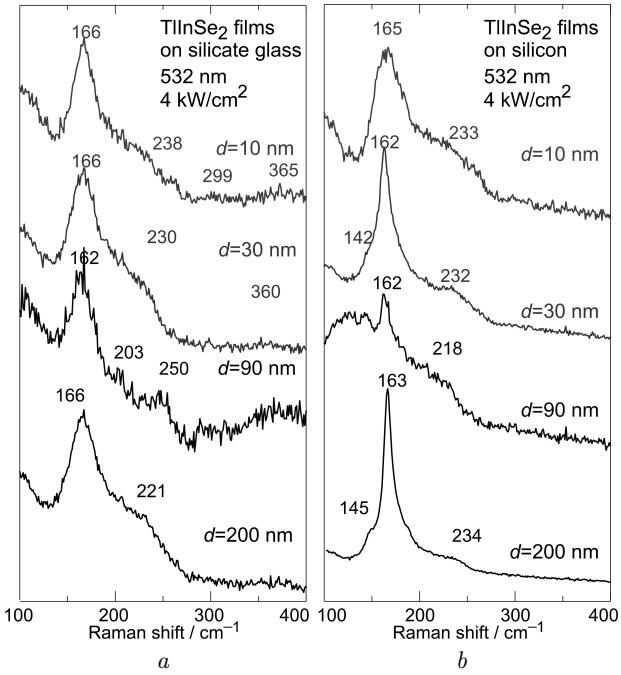


***Fig. 1.*** Micro-Raman spectra of $TlInSe_2$ films of different thicknesses $d$, thermally evaporated on silicate glass ($a$) and silicon ($b$) substrates. The spectra were measured at the excitation with $\lambda_{exc} = 532$ nm and $P_{exc} = 4$ kW/$cm^2$

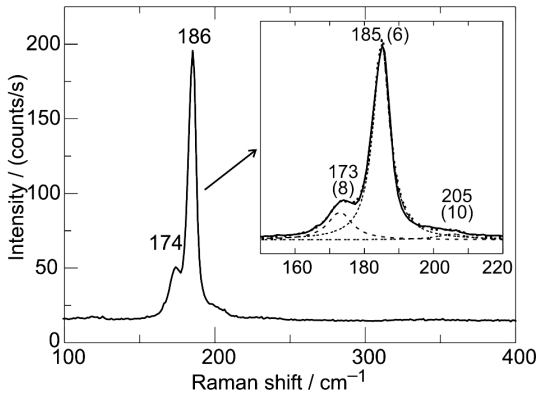


***Fig. 2.*** Micro-Raman spectra of a single-crystal $TlInSe_2$ sample in $Z(XX+XY)\bar{Z}$ scattering geometry measured at the excitation with $\lambda_{exc} = 532$ nm and $P_{exc} = 40$ kW/$cm^2$. The inset shows the simulation of the observed Raman spectrum by three Lorentzian contours, the frequency positions and half-widths (in parentheses) being indicated

In the case of $TlInSe_2$ films (Fig. 1), the absence of peaks close to the mentioned frequencies means the absence of clearly defined $TlInSe_2$ structural groups in the film (i.e., their amorphous character), while

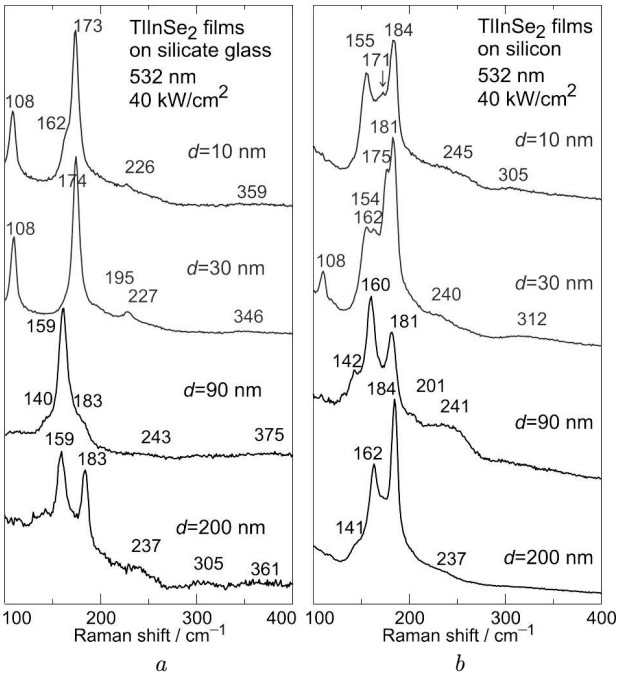


***Fig. 3.*** Micro-Raman spectra of $TlInSe_2$ films of different thicknesses $d$, thermally evaporated on silicate glass ($a$) and silicon ($b$) substrates. The spectra were measured at the excitation with $\lambda_{exc} = 532$ nm and $P_{exc} = 40$ kW/cm$^2$

the most intense peak near 165 cm$^{-1}$ corresponds to the vibrations of Tl–Se bonds in the amorphous film structure. Such feature is known to be observed in the Raman spectra of TlSe crystals [27] and thin films [28]. Meanwhile, In–Se bonds in the spectra of the amorphous films contribute to a broad continuum-like structure in the interval 200–250 cm$^{-1}$ (Fig. 1). An intense broad band in this spectral interval is reported for amorphous $In_2Se_3$ films [29].

Evidently, the reason for why, in our case, contrary to the recent studies of other groups [16, 17], the thermal evaporation resulted in amorphous $TlInSe_2$ films, is related to the substrate temperature. The authors of Refs. [16, 17] evaporated the films on substrates heated to 300–350 °C and obtained polycrystalline $TlInSe_2$ films, their structure being clearly confirmed by the X-ray diffraction and Raman spectroscopy. Meanwhile, in our case, the evaporation was performed onto cold substrates, and amorphous $TlInSe_2$ films were obtained.

Raman measurements performed for the same $TlInSe_2$ film samples at an increased $P_{exc} = 40$ kW/cm$^2$ (Fig. 3) revealed intense narrow maxima which clearly indicates a fast crystallization of the film material in the laser spot. Contrary to the low-$P_{exc}$ spectra which look much similar for the samples prepared at different substrates and with different film thicknesses (Fig. 1), the spectra measured at $P_{exc} = 40$ kW/cm$^2$ exhibit different peaks depending on the film thickness and the substrate type. The dependences are not always clearly defined, but some general trends can be pointed out.

Unpolarized room-temperature Raman spectra of crystalline $TlInSe_2$ in this frequency interval [8, 14], similarly to the spectrum shown in Fig. 2, demonstrate the most intense $A_{1g}$ symmetry peak at 183–186 cm$^{-1}$ and another one of $E_g$ symmetry at 171–173 cm$^{-1}$ which is weaker by about an order of magnitude [8,14]. In the films under investigation, the peak at 181–184 cm$^{-1}$ is observed for films of all thicknesses on the silicon substrates and for the thickest (200 nm) film on the silicate glass substrate. Meanwhile, the $E_g$ band at 171–175 cm$^{-1}$ is revealed only for thinner films (10–30 nm): for the films on the silicate glass substrate, it is the predominant peak in the spectra; while for the samples on the silicon substrate, it is only slightly weaker than the strongest peak at 181–184 cm$^{-1}$ (Fig. 3). Such behavior means that, for these films, the $TlInSe_2$ crystallites formed in the laser spot are not randomly oriented, because otherwise the ratio of the intensities of two bands in the spectrum would be close to that in the unpolarized spectrum of crystalline $TlInSe_2$. Note that, due to the chain-like structure of $TlInSe_2$, its nanocrystallites are known to be of elongated, rod-like shape [3, 12]. According to the group-theoretic analysis [2], the vibration of $E_g$ symmetry (171–175 cm$^{-1}$) corresponds to the *(XZ)* and *(YZ)* components of the Raman tensor. Taking into account the backscattering configuration, the observed preferential contribution from these components means that the $TlInSe_2$ nanorods should be oriented with the $Z$ direction (the nanorod axis) mostly within the film plane. Evidently, the restriction of the in-plane orientation of the nanorods was imposed by the small (10–30 nm) film thickness, since for thicker films the intensity of the $E_g$ band at 171–175 cm$^{-1}$ is negligible (Fig. 3) meaning that, in this case, the $TlInSe_2$ crystallites formed in the laser spot are randomly oriented.

However, besides the discussed $TlInSe_2$ peaks, there are more narrow features formed in the $TlInSe_2$ films and revealed in the spectra under the illumi-

nation with $P_{exc} = 40$ kW/cm$^2$. The most intense are the peaks at 155–160 cm$^{-1}$ and 108 cm$^{-1}$ (the latter is observed only for the films of smaller thicknesses). The peak near 160 cm$^{-1}$ is known to be the most prominent Raman feature of crystalline TlSe [27], while the one at 104 cm$^{-1}$ was reported as the most intense feature of $\alpha$-$In_2Se_3$ crystal [30]. It can be concluded that the high-$P_{exc}$ illumination leads to the formation of not only $TlInSe_2$, but also TlSe and $In_2Se_3$ crystallites in the illuminated area of the amorphous $TlInSe_2$ films.

The earlier formation of $TlInSe_2$ crystallites under the intense laser illumination was reported for Tl–In–As–Se glass [31] similarly to the formation of other chalcogenide nanocrystals in amorphous $As_2Se_3$-based films [32, 33]. In all cases, Raman spectroscopy was used to confirm the crystallite formation. It is essential that, in all those cases, the mechanism of this photoinduced effect is mostly nonthermal, based on a drastic drop of the material viscosity caused by the local photofluidization due to the interaction of the tightly focused laser beam with the amorphous $As_2Se_3$-based material. Note that, for those materials, the accompanying photoinduced effect of mass transport from a heavily illuminated area was revealed as the formation of a pit in the laser spot on the film surface [31–33].

In our case, on the contrary, we did not observe any damage on the film surface after the illumination and the Raman measurement. From this, we conclude that the formation of crystallites in the films in the course of the Raman measurement at the elevated $P_{exc}$ is driven by a thermal mechanism: the sample surface in the laser spot is heated by the tightly focused laser beam and thermally enhanced mobility enables the localized crystallite formation.

In order to check whether the structural changes in the $TlInSe_2$ films leading to the observed crystalline features emerging in their Raman spectra at a higher power density are indeed related to the thermal effect of the tightly focused laser beam, we performed the 30-min annealing of the $TlInSe_2$ film samples at 150 °C and 300 °C and subsequent measurements of their Raman spectra. The Raman measurements were performed at low $P_{exc} = 4$ kW/cm$^2$ to avoid an additional sample heating. The corresponding Raman spectra shown in Fig. 4 clearly reveal the intense sharp peaks emerging at 153–155 cm$^{-1}$ and 181–185 cm$^{-1}$, as well as a less pronounced feature at

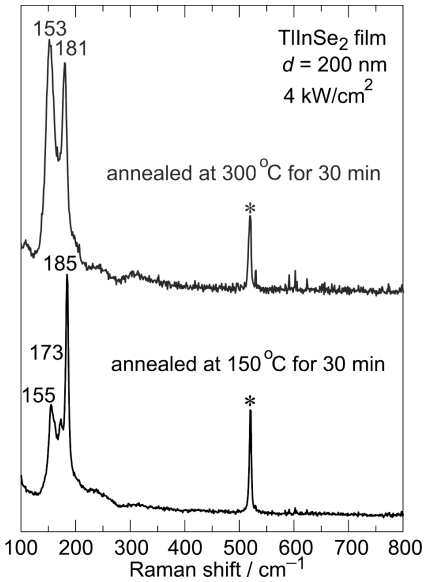


***Fig. 4.*** Micro-Raman spectra of $TlInSe_2$ films with the thickness $d = 200$ nm on silicon substrates annealed for 30 min at 150 °C and 300 °C. The spectra were measured at the excitation with $\lambda_{exc} = 532$ nm and $P_{exc} = 4$ kW/cm$^2$. Asterisks mark the 521 cm$^{-1}$ peak from the Si substrate

173 cm$^{-1}$. In view of the above discussion, it is quite reasonable to relate the peak at 153–155 cm$^{-1}$ to the TlSe crystallites and the features at 173 cm$^{-1}$ and 181–185 cm$^{-1}$ to the $TlInSe_2$ crystallites which evidently appear in the sample after the annealing. The spectra of the thermally annealed samples strongly resemble those of the untreated $TlInSe_2$ films measured at the higher $P_{exc} = 40$ kW/cm$^2$ (Fig. 3). These data clearly confirm that the crystallization effects revealed for the $TlInSe_2$ films under the higher $P_{exc}$ illumination result from the thermal effect of the focused laser beam.

## 4. Conclusions

$TlInSe_2$ films with thickness from 10 to 200 nm are prepared by the thermal evaporation on silicon and silicate glass substrates. Micro-Raman spectra measured at $\lambda_{exc} = 532$ nm and the moderate excitation power density $P_{exc} = 4$ kW/cm$^2$ show the dominating contribution from Tl–Se bond vibrations and confirm the amorphous character of the films.

At the elevated power density 40 kW/cm$^2$, narrow features emerge in the spectra, showing the evidence for the formation of $TlInSe_2$ as well as

TlSe and $In_2Se_3$ crystallites in the laser spot on the film surface. Based on the peak intensities, it is shown that, for thin (10–30 nm) films, the rod-shaped $TlInSe_2$ crystallites are oriented within the film plane. The formation of the crystallites is explained by the thermal effect of the tightly focused laser beam facilitating the mobility of atoms in the illuminated area. This conclusion is confirmed by the Raman measurements performed for the $TlInSe_2$ films annealed for 30 min at 150 and 300 °C which show the appearance of remarkably similar crystallite-related peaks.


1. D. Müller, G. Eulenberger, H.Z. Hahn. Thalliumchalkogenide mit Thalliumselenidstruktur. *Anorg. Allg. Chem. B.* **398**, 207 (1973).
2. N.M. Gasanly, A.F. Goncharov, B.M. Dzhavadov *et al.* Vibrational spectra of $TlGaTe_2$, $TlInTe_2$, and $TlInSe_2$ layer single crystals. *Phys. Status Solidi B* **97**, 367 (1980).
3. N. Mamedov, K. Wakita, A. Ashida *et al.* Super thermoelectric power of one-dimensional $TlInSe_2$. *Thin Solid Films* **499**, 275 (2006).
4. K. Mimura, K. Wakita, M. Arita *et al.* Angle-resolved photoemission study of quasi one-dimensional $TlInSe_2$. *J. Electron Spectrosc. Related Phenom.* **156–158**, 379 (2007).
5. G. Orudzhev, V. Jafarova, S. Schorr *et al.* Phonon spectra of chain TlSe and $TlInSe_2$: Density functional theory based study. *Jpn. J. Appl. Phys.* **47**, 8193 (2008).
6. A.F. Qasrawi, N.M. Gasanly. Transient and steady state photoelectronic analysis in $TlInSe_2$ crystals. *Mater. Res. Bull.* **46**, 1227 (2011).
7. A.F. Qasrawi, N.M. Gasanly. Mixed conduction and anisotropic single oscillator parameters in low dimensional $TlInSe_2$ crystals. *Mater. Chem. Phys.* **141**, 63 (2013).
8. N. Kalkan, S. Celik, H. Bas, A.E. Ozel. Conduction mechanisms, molecular modelling and micro-Raman studies of $TlInSe_2$ chalcogenide crystal. *J. Optoelectron. Adv. Mater.* **19**, 234 (2017).
9. S. Hosokawa, J. R. Stellhorn, H. Ikemoto *et al.* Lattice distortions in $TlInSe_2$ thermoelectric material studied by X-ray absorption fine structure. *Phys. Status Solidi B* **215**, 1700416 (2018).
10. A.M. Panich. Electronic properties and phase transitions in low-dimensional semiconductors. *J. Phys.: Condens. Matter* **20**, 293202 (2008).
11. I. Martynyuk-Lototska, O. Mys, A. Say *et al.* Anisotropy of acoustic and thermal expansion properties of $TlInSe_2$ crystals. *Phase Transit.* **92**, 23 (2019).
12. N. Mamedov, K. Wakita, S. Akita, Y. Nakayama. 1D-$TlInSe_2$: Band structure, dielectric function and nanorods. *Jpn. J. Appl. Phys.* **44**, 709 (2005).
13. A.F. Qasrawi, F.G. Aljammal, N.M. Taleb, N.M. Gasanly. Design and characterization of $TlInSe_2$ varactor devices. *Physica B* **406**, 2740 (2011).
14. A.V. Gomonnai, I. Petryshynets, Yu.M. Azhniuk *et al.* Growth and characterisation of sulphur-rich $TlIn(S_{1-x}Se_x)_2$ single crystals. *J. Crystal Growth.* **367**, 35 (2013).
15. O.O. Gomonnai, M. Ludemann, A.V. Gomonnai *et al.* Low-temperature Raman studies of sulfur-rich $TlIn(S_{1-x}Se_x)_2$ single crystals. *Vibr. Spectrosc.* **97**, 114 (2018).
16. S.A. Al-Ghamdi, A.A.A. Darwish, T.A. Hamdalla *et al.* Structural analysis, dielectric relaxation, and AC electrical conductivity in $TlInSe_2$ thin films as a function of temperature and frequency. *Opt. Mater.* **129**, 112514 (2022).
17. F.F. Al-Harbi, A.A.A. Darwish, T.A. Hamdalla, K.F. Abd El-Rahman. Structural analysis, dielectric relaxation, and AC electrical conductivity in $TlInSe_2$ thin films as a function of temperature and frequency. *Appl. Phys. A* **128**, 622 (2022).
18. S.N. Mustafaeva, M.M. Asadov, K.Sh. Qahramanov. Frequency-dependent dielectric coefficients of $TlInS_2$ amorphous films. *Semicond. Phys., Quantum Electron. Optoelectron.* **10**, 58 (2007).
19. M.M. El-Nahass, H.M. Zeyada, N.A. El-Ghamaz, A. El-Ghandour Shetiwy. Particle size reduction of thallium indium disulphide nanostructured thin films due to post annealing. *Optik.* **171**, 580 (2018).
20. B.A. Ünlü, A. Karatay, M. Yüksek *et al.* The effect of Ga/In ratio and annealing temperature on the nonlinear absorption behaviors in amorphous $TlGa_xIn_{(1-x)}S_2$ ($0 \leq \leq x \leq 1$) chalcogenide thin films. *Opt. Laser Technol.* **128**, 106230 (2020).
21. I. Guler, N. Gasanly. Structural and optical properties of thermally annealed thallium indium disulfide thin films. *Thin Solid Films* **704**, 137985 (2020).
22. B.A. Ünlü, A. Karatay, E.A. Yildiz *et al.* Defect assisted nonlinear absorption and optical limiting in amorphous $TlGaS_{2(1-x)}Se_{2(x)}$ ($0 \leq x \leq 1$) chalcogenide thin films. *J. Luminesc.* **241**, 118540 (2022).
23. Y.M. Azhniuk, A.V. Gomonnai, D. Solonenko *et al.* Characterization of Ag–In–S films prepared by thermal evaporation. *Mater. Today Proc.* **62**, Pt. 9, 5745 (2022).
24. M. Isik, A. Karatay, N.M. Gasanly. Structural and optical characteristics of thermally evaporated $TlGaSe_2$ thin films. Opt. Mater. **124**, 112018 (2022).
25. Y.M. Azhniuk, A.V. Gomonnai, D. Solonenko *et al.* Raman and X-ray diffraction study of Ag–In–S polycrystals, films, and nanoparticles. *J. Mater. Res.* **38**, 2239 (2023).
26. I. Guler, M. Isik, N. Gasanly. Structural and optical properties of $(TlInS_2)_{0.75}(TlInSe_2)_{0.25}$ thin films deposited by thermal evaporation. *J. Mater. Sci.: Mater. Electron.* **34**, 177 (2023).

27. J. Zirke, G. Frahm, A. Tausend, D. Wobig. Infrared and Raman studies of TlSe. *Phys. Status Solidi B* **75**, K149 (1976).
28. A.E. Ozel, D. Deger, S. Celik *et al.* Dielectric and Raman spectroscopy of TlSe thin films. *Physica B* **527**, 72 (2017).
29. J. Weszka, Ph. Daniel, A. Burian *et al.* Raman scattering in $In_2Se_3$ and $InSe_2$ amorphous films. *J. Non-Cryst. Solids* **265**, 98 (2000).
30. R. Lewandowska, R. Bacewicz, J. Filipowicz, W. Paszkowicz. Raman scattering in $\alpha$-$In_2Se_3$ crystals. *Mater. Res. Bull.* **36**, 2577 (2001).
31. Y.M. Azhniuk, A.V. Gomonnai, V.M. Rubish *et al. In situ* Raman observation of laser-induced formation of $TlInSe_2$ crystallites in Tl–In–As–Se glass. *J. Phys. Chem. Solids* **74**, 1452 (2013).
32. Y.M. Azhniuk, D. Solonenko, V.Yu. Loya *et al.* Flexoelectric and local heating effects on CdSe nanocrystals in amorphous $As_2Se_3$ films. *Mater. Res. Expr.* **6**, 095913 (2019).
33. Y.M. Azhniuk, V.V. Lopushansky, V.Yu. Loya *et al.* Raman study of laser-induced formation of II–VI nanocrystals in zinc-doped As–S(Se) films. *Appl. Nanosci.* **10**, 4831 (2020).

Received 21.10.23

*Ю. Ажнюк, О.В. Гомоннай, В. Лопушанський, О.О. Гомоннай, Т. Бабука, В. Лоя, І. Войнарович*

РАМАНІВСЬКЕ ДОСЛІДЖЕННЯ ІНДУКОВАНИХ ЛАЗЕРНИМ ВИПРОМІНЮВАННЯМ ПЕРЕТВОРЕНЬ У ТЕРМІЧНО НАПИЛЕНИХ ТОНКИХ ПЛІВКАХ $TlInSe_2$

Плівки $TlInSe_2$ товщиною від 10 до 200 нм отримано термічним напиленням на підкладинки з кремнію та силікатного скла, що перебували при кімнатній температурі. Мікрораманівські спектри, виміряні при помірній густині потужності збудження (532 нм, 4 кВт/см$^2$), підтверджують аморфний характер отриманих плівок. При підвищенні густини потужності до 40 кВт/см$^2$ у спектрах з'являються вузькі лінії, спектральне положення яких вказує на формування кристалітів $TlInSe_2$, а також TlSe та $In_2Se_3$ у місці падіння лазерного променя на поверхню плівки. Показано, що для тонких (10–30 нм) плівок кристаліти $TlInSe_2$ мають видовжену форму і орієнтовані у площині плівки. Утворення кристалітів обумовлене локальним нагріванням плівки сильно сфокусованим лазерним пучком.

*Ключові слова*: тонкі плівки, термічне напилення, раманівська спектроскопія, кристалізація.